

Metal–Organic Frameworks Capable of Healing at Low Temperatures

Ziguang Chen, Gonghua Wang, Zhanping Xu, Hui Li, Alexandre Dhôtel, Xiao Cheng Zeng, Banglin Chen, Jean-Marc Saiter, and Li Tan*

Metal–organic frameworks (MOFs) are crystalline materials with large lattice parameters that afford them organized pores spacious enough to trap small molecules of gases for energy storage^[1] or oligomers for drug delivery.^[2] In contrast to other types of porous materials, such as silicates^[3] or crosslinked polymer networks,^[4] which have constituent components that interact mainly through covalent bonds, the slightly ionic nature of the building blocks in MOFs makes these solid frameworks vulnerable or dynamic when exposed to a polar liquid environment. For example, organic linkers in MOFs can be replaced by simply soaking the crystals in a fresh ionic solution^[5–7]; the exchange of metal centers in frameworks allows the synthesis of alloy-like solids^[7,8]; the unloading of organic linkers triggers a sustained robotic motion in liquid/air interface^[9]; and the transformation of shiny crystals into hairy ones facilitates sequential trapping of proteins.^[10] Nevertheless, these interesting phenomena all suggest extreme dynamic or chemical instability of framework structures. Is there any way to reverse this process or to heal the corroded crystals by patching the escaped building blocks back to the original framework structure? Since extensive research or designs in MOFs have been geared towards heterogeneous catalysis in chemical reactors, healing of these crystalline solids will undoubtedly extend their operation lifetime; when inter-solid healing or binding is made possible, dense packing could even promote the toughness of the solid, facilitating multiple cycles of loading and unloading.

Moreover, many efforts in these artificial crystals have been placed on constructing unique bulk crystalline structures, while very little attention has been paid to the outer surfaces

of the solids. Since MOFs share similar mechanical behavior to rigid solids of ceramics, a lack of rotational freedom in their stacking^[12] or a slight variation in crystal growth could yield many small crystal grains atop the solid surfaces. When an uneven volume change or a crack is initiated, it could lead to catastrophic failure over a short period of time. Will the proposed healing effectively weld the small grains into larger ones? While we know eutectic solids can weld at a lower temperature than their individual components alone,^[12] phase transitions in many metal-containing solids or oxides occur at a temperature way beyond the service conditions available.^[12] If rather low interface mobility from the atomic or ionic constituents has hindered the interfacial regroupings, will a stronger mobility from MOFs effectively lower the resulting temperature in healing?

To shed light on the aforementioned questions, we report our work in healing crystalline solids of MOFs, where tiny grains on bulk solid surfaces can merge into larger ones at a temperature of $-56\text{ }^{\circ}\text{C}$ (which is $45\text{ }^{\circ}\text{C}$ lower than that of eutectic solids of Na/K^[13] and $80\text{ }^{\circ}\text{C}$ lower than room temperature synthesis of one recent MOFs).^[14] When our MOFs are crushed into powders, the resultant solid membranes show enhanced toughness or bendability after healing; when pristine crystals are healed, a 300% leap in modulus and 250% in hardness are observed. In particular, we chose Cu-MOFs (Cu(FMA)(4,4'-Bpe)_{0.5}·0.5H₂O)^[15] that were synthesized with an interpenetrating pseudo-cubic crystal structure (Figure S1, Table S2, Supporting Information) to demonstrate our healing concept. Before any healing process is allowed to occur, these MOFs are briefly dispersed or soaked in water. Once a sufficient amount of building blocks have been released into this polar medium, water is removed by natural drying and diethylformamide (DEF, (C₂H₅)₂NCOH) is added as the healing agent. **Figure 1A** demonstrates the healing of a broken elastic membrane by applying crushed powders of these MOFs. When the elastic membrane was cut with a blade (Figure 1A, left), the open wound was briefly treated with DEF. Shortly after, the membrane recovered most of its bendability in ambient conditions (Figure 1A, right). Another freestanding leaf-like structure molded from MOF powders (Figure 1B) was even capable of withstanding a high temperature up to $200\text{ }^{\circ}\text{C}$ without a major breakdown. Both microscopic (nanoindentation) and macroscopic experiments (three-point bending) were utilized to evaluate the membrane before and after the DEF treatment (Figure 1C). As the nanoindentation load increased, the physically aggregated membrane behaved in a rather fragile manner (Figure 1C, upper inset), and failure marks on the loading curve suggest easy and permanent deformations. By contrast, the healed membrane

Dr. Z. Chen, Dr. G. Wang, Z. Xu, A. Dhôtel, Prof. L. Tan
Department of Mechanical and Materials Engineering

University of Nebraska
Lincoln, Nebraska, 68588, USA
Email: ltan4@unl.edu

Dr. H. Li, Prof. X. C. Zeng
Department of Chemistry
University of Nebraska
Lincoln, Nebraska, 68588, USA

A. Dhôtel, Prof. J.-M. Saiter
AMME–LECAP, EA4528
International Laboratory
Institut des Matériaux de Rouen
Université et INSA de Rouen

BP12, Saint Etienne du Rouvray Cedex, 76801, France

Prof. B. Chen
Department of Chemistry
University of Texas at San Antonio
One UTSA Circle, San Antonio, Texas, 78249, USA



DOI: 10.1002/adma.201302471

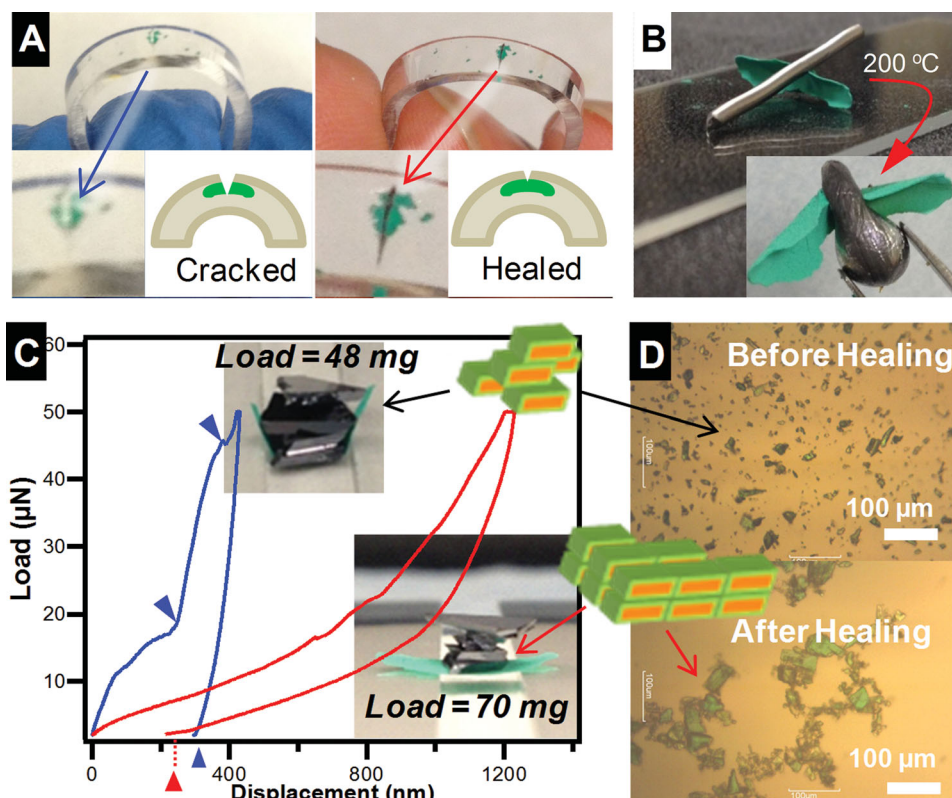


Figure 1. Mechanically crushed Cu-MOFs powders capable of healing at ambient conditions. A) Snapshots and schematics of a MOF/polydimethylsiloxane (PDMS) composite showing the diminished wound after DEF treatment. B) MOF can be molded into a freestanding 3D object by keeping the shape even after annealing at 200 °C, at which a solder rod melts. C) Typical load-displacement curves of the MOF membranes before (blue) and after (red) healing. Failures of the unbound membrane are marked by blue triangles. The picture insets record the maximum loadings (48 vs 70 mg) that the membranes (unbound vs bound) bear in a three-point bending test. D) Optical microscope images of well dispersed MOF crystals in water (top) and the highly networked ones after DEF addition (bottom).

easily deflected with a smooth loading curve by retaining little residual strain. On closer inspection of the crushed pieces of these crystals, it could be seen that they were loosely dispersed in water and that their morphologies remained intact for extended periods of time (Figure 1D). After addition of DEF, dispersed solids immediately bundled together by forming network-like aggregates, providing evidence of the anisotropic nature of Cu-MOFs during this healing process.

We can gauge this anisotropy from the Cu-MOFs by looking at the compositions of their major crystal planes (Table S2, Supporting Information). The frameworks are essentially organized via noncovalent bonding of either copper and oxygen (Cu–O) or copper and nitrogen (Cu–N), where the latter is a much weaker bond than the former.^[16] As a consequence, the (200) planes have the lowest interlayer strength, indicating a low driving force to form the bonds or less stability. If we crush a bulk crystal of such into fine pieces, we would expect the outer surfaces of the powders to be mainly (200) planes. Indeed, atomic force microscopy (AFM) scanning revealed layered structures with individual layer thickness of 0.77 nm, closely matching 0.80 nm of lattice spacing for (200) planes (Figure 2A,B). The dynamic changes on this (200) plane were caught after soaking the sample in water and were supported by in situ AFM imaging at different times (Figure 2C,D). Immediately after water covered the crystal surface, many small

holes appeared; after 17 minutes, these holes became deeper and larger (as marked by the red ovals and yellow rectangles in Figure 2D), indicating a continuous dissolution of substances from the surfaces into the aqueous medium. When the water-soluble substance was extracted, ¹H NMR confirmed the existence of fumarate (s, d = 6.7 ppm), as shown in Figure 2E. Collectively, both the AFM and NMR studies point to one fact: the water-soluble fumaric acid or fumarate moieties roll off from (200) surfaces, destabilizing the Cu-MOFs crystal in a continuous manner. Naturally, this presents questions about the role of the liquid, DEF, in the healing process. A brief comparison of the diffraction patterns of crushed solids before and after DEF treatment suggests peak sharpening at (200) surfaces only (Figure 2F and Table S2, Supporting Information). Since the peak intensity or sharpness is indicative of the perfectness of the inter-planar stacking, a sharper (200) peak unambiguously indicates a promoted crystal alignment and structure perfection along the [200] direction (Table S1, Supporting Information).

Even though DEF can patch fresh (200) surfaces with building blocks (fumarate), an energy release is still required to ensure the tight connection between (200) surfaces. Since the Cu-MOFs were synthesized from an aqueous environment, it is not surprising that the exposed (200) surfaces are covered with a thin layer of water molecules (in green, Figure 3A). Viewing these surfaces carefully suggests that the water molecules are

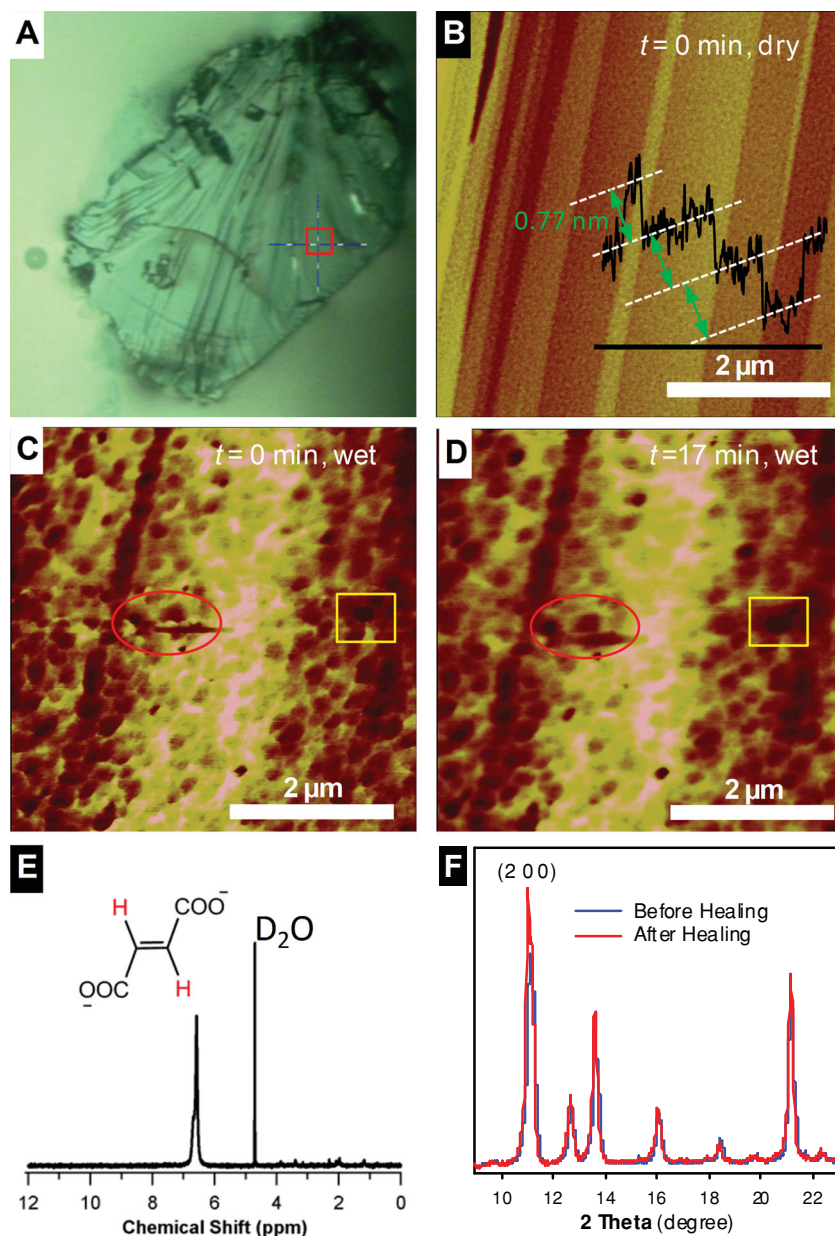


Figure 2. Surface morphology of one piece of crushed Cu-MOFs and its dynamic evolution in liquid. A) Optical microscope image of the crushed crystal with dense surface terrains. B) AFM image revealing the surface terraces with a fringe spacing of approximately 0.77 nm, matching the interplanar distance of (200) planes. C–D) AFM images recording the morphological evolution of the water-soaked surface at 0 and 17 min. E) ^1H NMR spectrum of the clear solution filtered from a mixture of MOF powders and D_2O after a 24-hour impregnation. F) Powder XRD pattern of the MOF powders before and after DEF treatment.

largely contained between the top boundaries of the (200) surfaces only, creating a pseudo-stable configuration. As water is not a good solvent for dangling building blocks (4,4'-Bpe), the presence of water layer alone blocks the diffusion of these 4,4'-Bpe and inhibits the binding of (200) surfaces. When amphiphilic molecules (DEF in Figure 3B, red sticks) are poured into this system, the nonpolar branches (two ethyl groups) from the DEF are quickly inserted in between the (200) planes by depleting the surface water and also distorting the surface

framework to a certain degree (Figure 3B). Essentially, strong affinity of the surface components to bipolar molecules such as DEF has destabilized the original surface configuration. As a result, a large energy release from this DEF engagement is likely to promote Cu–N restructuring or the binding of Cu and the dangling 4,4'-Bpe. As evidenced by our experiment shown in Figure 3C and Figure S2, Supporting Information, water vapors from the Cu-MOFs/water/DEF mixture were frequently caught, suggesting that local heating is a plausible mechanism for the observed binding. Another piece of evidence is revealed as water-dispersed solids were mixed with a few droplets of DEF: quick vibrations of the solids followed by an immediate networking were recorded (Figure S3, left panel, Supporting Information). While liquid diffusion around the solids can introduce a certain level of dynamic fluctuation, the long-lasting vibration is perhaps closely related to the local heat release (Figure S3, right panel, Supporting Information). Essentially, this local heating has driven off the water molecules from the cleaved (200) planes and mobilized the metal centers or organic linkers. It is worth noting that this DEF-assisted interfacial binding is different from the traditional solvent exchange or extraction/insertion processes.^[6] As the DEF molecule (4.5 Å) is considerably larger than the pore size of Cu-MOFs (3.6 Å),^[15] it will not intrude the bulk frameworks. Correspondingly, we observed only a relative change in peak intensities on X-ray diffraction (XRD) with no alteration in any of the peak positions.

While defects or dangling bonds can be created mechanically or by solvation in an aqueous environment, freshly synthesized MOF crystals are not perfect either. If crushed solids or powders can heal, this process might even repair defects on as-synthesized bulk crystals (Figure 4). We used nanoindentation as an effective tool to evaluate binding-induced healing in surface deformation. Unlike mechanical tests for crushed membranes in Figure 1C, neither of our samples here showed permanent deformation: rather, smooth curves were observed in both loading and unloading regions, where the modulus jumped from 4 to 12 GPa and hardness from 400 to 1000 MPa. Since the statistical plot in Figure 4B suggests that this as a general trend, we tend to believe that this healing or welding process once again closely resulted from structure transition on surfaces. As revealed in Figure 4C, before surface healing, the Cu-MOFs surface was composed of many small grains with an average size of 10 nm; after healing, the average diameter increased

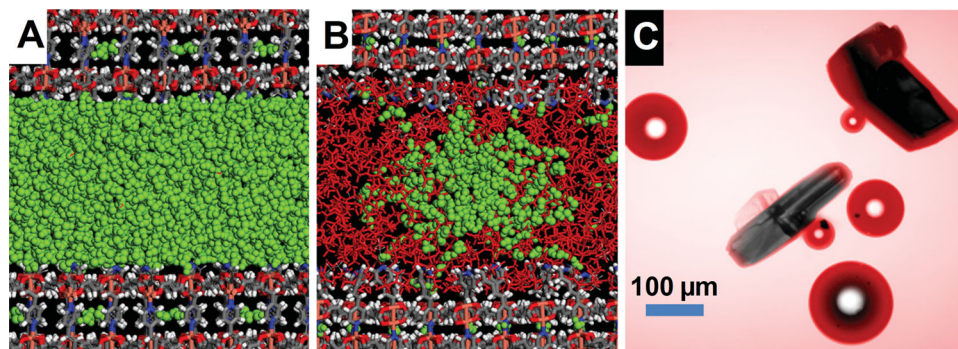


Figure 3. Molecular dynamics simulation of the interfacial healing process and optical image of bubbles generated during the DEF treatment. A) Ball and stick model of water molecules on the (200) surface of Cu-MOFs. B) Structure model of water dewetting on (200) after DEF is involved. Water molecules are represented as green balls and DEF as red sticks. C) Laser scanning confocal microscope image capturing water bubbles adjacent to the bulk crystal of MOFs after DEF incorporation at room temperature. Fluorescent dye is used in the imaging process for visual convenience.

drastically to 30 nm. The XRD patterns (Figure 4D) before and after this transition suggest this merging occurs mostly in (200) and (002) planes, as evidenced by the peak sharpening and also the increased domain sizes estimated from Scherrer's equation (Table S1, Supporting Information). When crystal grain size increases, the surface area and the surface defect density

decrease, rendering less scattering in measurement (Figure 4B, upper corner) and a much-enhanced mechanical performance.

From the structure point of view, the surface healing or welding has tightened the dangling Cu–N bonds on the MOFs surfaces. As illustrated in Figure S4, Supporting Information, MOF crystals bear a heterogeneous layered structure. We

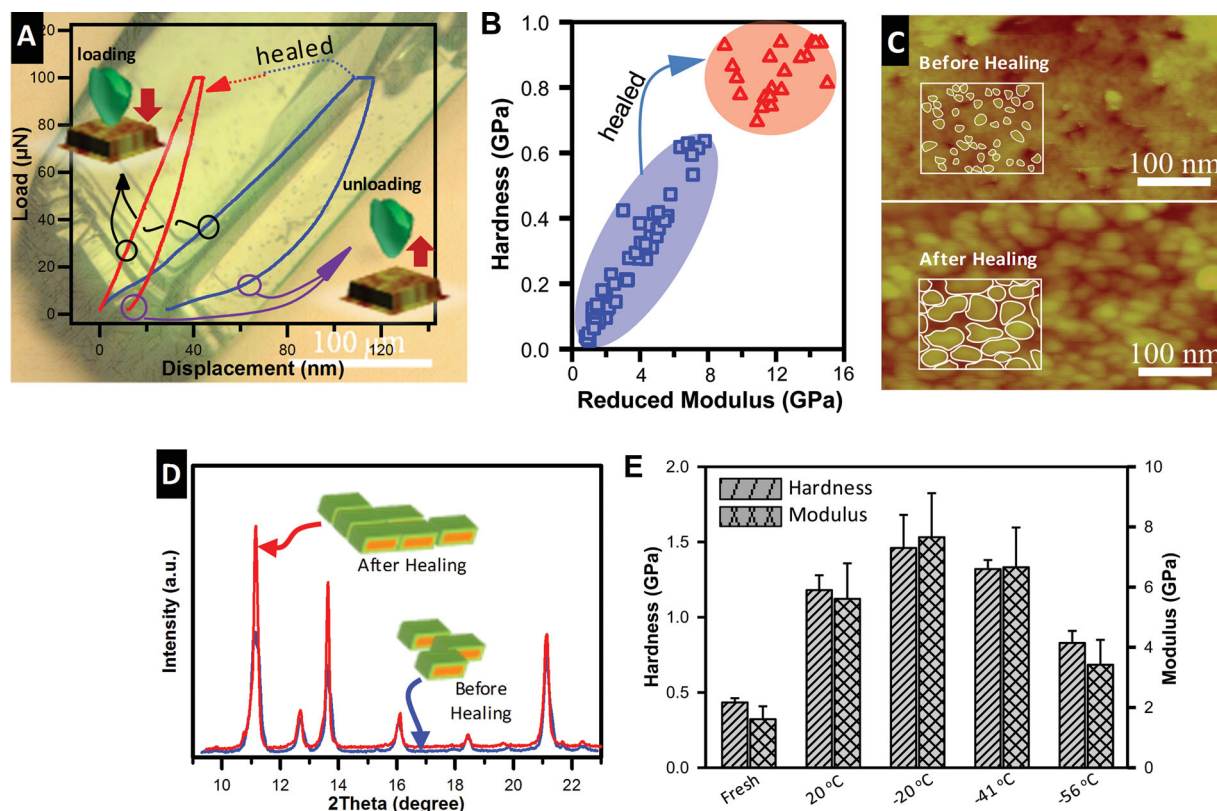


Figure 4. Bulk crystal of Cu-MOFs capable of surface healing. A) Load-displacement curves of the fresh and bound MOF crystals; the optical image of one crystal is set as background. B) Hardness-reduced modulus plot of the nanoindentation results of the fresh (blue) and repaired (red) crystals, revealing a statistical leap in deformation resistance. C) Powder XRD patterns of the fresh and repaired crystals. D) AFM images of the crystal surfaces showing increased grain sizes after surface healing. E) Modulus and hardness histograms extracted from groups of nanoindentation, showing enhanced mechanical properties after healing at low temperatures. Note: cold DEF at -20 , -41 , and -56 °C was obtained by placing glass vials containing DEF in a cold bath of sodium chloride/ice ($w/w = 1/3$), acetonitrile/dry ice, and octane/dry ice, respectively.

postulate $\langle 022 \rangle$ to be the preferred orientation for bulk crystals, where each (022) of the unit cell contains 8 Cu–O and 4 Cu–N bonds. As evidenced by Figure S4B, Supporting Information, abundant defects or etch pits are clearly visible all over the (022), giving us the opportunity to see repaired surfaces with much increased grain sizes (Figure 4C). However, if those tiny grains are merged through the Cu–N directions only, then longitudinal shaped or rod-like larger grains are expected. By contrast, what we saw in Figure 4C were rounded grains, suggesting that merging occurs in more than one direction or that healing of Cu–O bonds occurs too. Indeed, the XRD patterns (Figure 4D) for DEF-treated bulk crystals show peak sharpening for both (200) and (002) planes. If we recall that Cu–N and Cu–O are the respective backbones along these two directions (Figure S1, Supporting Information), this finding extends the dynamic binding from Cu–N to Cu–O, even though the former is much easier to obtain and to engineer.

To explore low-temperature healing or welding, we soaked fresh crystals of Cu-MOFs in cold baths of DEF at various low temperatures (-20 , -41 , and -56 °C). We evaluated the surface healing on crystal alignment, grain size, and mechanical properties. Likewise, the diffraction peak of (200) planes became sharper even after a cold bath treatment at -56 °C (Figure S5, Supporting Information), where average grain size increased from 15 to 25 nm, accompanied by nearly doubled mechanical properties (Figure 4E). By comparison, soaking at a slight higher temperature of either -20 or -41 °C has tripled the hardness and modulus (Figure 4E). While the latter ones are not hugely different from those obtained in the ambient condition, a substantial viscosity increase in DEF at -56 °C has limited the diffusion of fumarate for reattachment of surface dangling bonds. Nonetheless, these experiments suggest that low temperatures do not restrict the healing between crystalline gaps. It is worthwhile noting that there are already a few reports of room temperature synthesis of MOFs using liquid phase epitaxy^[17] or spray drying methods.^[14,18] While we cannot exclude the possibility of executing these ambient processes at even lower temperatures, the energy need to patch a crystal is certainly not at the same level as the energy needed to assemble multiple types of building blocks for 3D stacking. Additionally, a lower temperature synthesis could occur at the expense of smaller crystals or much less surface areas. Furthermore, the healing agent DEF, which was used to patch imperfect crystals, is not just a solvent: its amphiphilic nature has a tendency to remove surface water molecules and therefore to lower the resistance for the acid linker (fumaric acid) to bond with the dangling base (4,4'-Bpe). As the latter process occurs with a thermal energy release, our patching is largely self-sustained. If those ambient syntheses follow a kinetic or thermal collision-dominant process, substantial resistance for a low-temperature assembly is then expected.

In conclusion, crystals of metal-organic frameworks (MOFs) can be destabilized in a polar liquid environment by releasing building blocks that can be further patched back through a healing process at ambient and low-temperature conditions. After healing, solid membranes exhibit greater mechanical resistance, which can potentially be molded into freestanding

3D objects or can mend broken elastic membranes. As patching crystalline gaps with small molecules largely drives these healing processes, sufficient mobility of the assisting reagents allows patching to happen at temperatures as low as -56 °C. If these healing phenomena are utilized for many other MOFs that are adopted as catalysts or as hydrogen storage or separation materials, we expect their structure integrity can be kept after multiple cycles of packing or extensive uses. Furthermore, the knowledge gained will help us design future crystalline solids or ordered structures that can be assembled, repaired, or healed in various engineering applications.

Experimental Section

Cu-MOFs Powders and Membranes: The powders were prepared by mechanically crushing as-synthesized Cu-MOFs crystals using a mortar and pestle. The Cu-MOFs membrane (>15 μm in thickness) for nanoindentation tests was obtained by drop-casting a 2.0 wt% water suspension of Cu-MOFs powders onto a piece of Si wafer. The Cu-MOFs membrane (≈ 25 μm in thickness) for a three-point bending test, however, was prepared by drop-casting 5.0 wt% Cu-MOFs powder suspension on a Teflon film. After water was naturally removed, a freestanding membrane was harvested directly from the Teflon substrate.

Healing of Cu-MOFs Membranes: The membrane for nanoindentation tests was obtained after dropping 0.2 mL of DEF ($>99.0\%$, TCI America) over crushed MOF powders on glass and let it dry in air. The healing of the membrane (freestanding) was achieved by soaking the freestanding piece in DEF for 12 hours.

Cu-MOFs/PDMS Composite: A bubble-free fresh PDMS precursor was casted atop a polycarbonate film to form a thin layer with a thickness of 1 mm. Crushed Cu-MOFs powders were then laid on this uncured PDMS surface, letting the solid sink to the bottom of the viscous liquid. The final Cu-MOFs/PDMS composite was received after annealing the mixture in the convection oven at 100 °C for 1 hour.

Micro- and Macro-scale Mechanical Tests: Nanoindentation tests were performed using Hyston Bio-Ubi. Quasi-static "trapezoidal" load function tests were selected that had a 5-s loading, a 2-s holding, and a final 5-s unloading. Maximum forces were set at 50 or 100 μN . The tip used is a Berkovich tip with a tip radius of 70 nm. In three-point bending tests, samples were placed between two glass slides with a spacing of 3 mm. Carefully weighted small Si pieces were then gradually loaded on top of each sample to investigate the maximum deflection before a failure.

Modeling Methods: A modified CVFF force field was used in the molecular dynamics (MD) simulations with flexible SPC model for water. The systems were equilibrated in the canonical ensemble at 300 K. The simulation time was 1.0 ns with a time interval of 1.0 fs. All the simulations were performed with the Discover module in the Material Studio package.

Supporting Information

Supporting Information is available from the Wiley Online Library or from the author.

Acknowledgements

The authors gratefully acknowledge the financial support from the US National Science Foundation, the Nebraska Center for Energy Science Research, and Layman New Directions (from the University of Nebraska–Lincoln (UNL)). L.T. appreciates the helpful discussions with Prof. Jian Zhang (UNL). H.L. and X.C.Z. thank the University of Nebraska

Holland Computing Center for providing computational resources with the associated USCMS Tier-2 site at UNL.

Received: May 30, 2013

Published online:

- [1] a) L. J. Murray, M. Dinca, J. R. Long, *Chem. Soc. Rev.* **2009**, *38*, 1294; b) M. P. Suh, H. J. Park, T. K. Prasad, D. W. Lim, *Chem. Rev.* **2012**, *112*, 782; c) M. Dinca, J. R. Long, *Angew. Chem. Int. Ed.* **2008**, *47*, 6766; d) N. L. Rosi, J. Eckert, M. Eddaoudi, D. T. Vodak, J. Kim, M. O'Keeffe, O. M. Yaghi, *Science* **2003**, *300*, 1127; e) J. L. C. Rowsell, O. M. Yaghi, *Angew. Chem. Int. Ed.* **2005**, *44*, 4670; f) B. Kesanli, Y. Cui, M. R. Smith, E. W. Bittner, B. C. Bockrath, W. B. Lin, *Angew. Chem. Int. Ed.* **2005**, *44*, 72; g) T. A. Makal, J. R. Li, W. G. Lu, H. C. Zhou, *Chem. Soc. Rev.* **2012**, *41*, 7761; h) J. Zhang, T. Wu, S. M. Chen, P. Y. Feng, X. H. Bu, *Angew. Chem. Int. Ed.* **2009**, *48*, 3486.
- [2] a) P. Horcajada, R. Gref, T. Baati, P. K. Allan, G. Maurin, P. Couvreur, G. Ferey, R. E. Morris, C. Serre, *Chem. Rev.* **2012**, *112*, 1232; b) H. X. Deng, S. Grunder, K. E. Cordova, C. Valente, H. Furukawa, M. Hmadeh, F. Gandara, A. C. Whalley, Z. Liu, S. Asahina, H. Kazumori, M. O'Keeffe, O. Terasaki, J. F. Stoddart, O. M. Yaghi, *Science* **2012**, *336*, 1018; c) P. Horcajada, C. Serre, M. Vallet-Regi, M. Sebban, F. Taulelle, G. Ferey, *Angew. Chem. Int. Ed.* **2006**, *45*, 5974; d) P. Horcajada, C. Serre, G. Maurin, N. A. Ramsahye, F. Balas, M. Vallet-Regi, M. Sebban, F. Taulelle, G. Ferey, *J. Am. Chem. Soc.* **2008**, *130*, 6774.
- [3] a) H. Yang, N. Coombs, G. A. Ozin, *Nature* **1997**, *386*, 692; b) D. Y. Zhao, J. L. Feng, Q. S. Huo, N. Melosh, G. H. Fredrickson, B. F. Chmelka, G. D. Stucky, *Science* **1998**, *279*, 548; c) A. Stein, B. J. Melde, R. C. Schroden, *Adv Mater* **2000**, *12*, 1403; d) Q. S. Huo, D. I. Margolese, U. Ciesla, P. Y. Feng, T. E. Gier, P. Sieger, R. Leon, P. M. Petroff, F. Schuth, G. D. Stucky, *Nature* **1994**, *368*, 317.
- [4] a) J. X. Jiang, F. Su, A. Trewin, C. D. Wood, N. L. Campbell, H. Niu, C. Dickinson, A. Y. Ganin, M. J. Rosseinsky, Y. Z. Khimyak, A. I. Cooper, *Angew. Chem. Int. Ed.* **2007**, *46*, 8574; b) J. Schmidt, M. Werner, A. Thomas, *Macromolecules* **2009**, *42*, 4426; c) R. Dawson, A. Laybourn, R. Clowes, Y. Z. Khimyak, D. J. Adams, A. I. Cooper, *Macromolecules* **2009**, *42*, 8809; d) X. F. Ji, Y. Yao, J. Y. Li, X. Z. Yan, F. H. Huang, *J. Am. Chem. Soc.* **2013**, *135*, 74; e) D. Q. Yuan, W. G. Lu, D. Zhao, H. C. Zhou, *Adv. Mater.* **2011**, *23*, 3723; f) W. G. Lu, J. P. Sculley, D. Q. Yuan, R. Krishna, Z. W. Wei, H. C. Zhou, *Angew. Chem. Int. Ed.* **2012**, *51*, 7480.
- [5] H. H. Fei, C. H. Pham, S. R. J. Oliver, *J. Am. Chem. Soc.* **2012**, *134*, 10729.
- [6] M. Kondo, S. Furukawa, K. Hirai, S. Kitagawa, *Angew. Chem. Int. Ed.* **2010**, *49*, 5327.
- [7] S. M. Cohen, *Chem. Rev.* **2012**, *112*, 970.
- [8] a) X. Song, S. Jeong, D. Kim, M. S. Lah, *Crystengcomm* **2012**, *14*, 5753; b) S. Das, H. Kim, K. Kim, *J. Am. Chem. Soc.* **2009**, *131*, 3814.
- [9] Y. Ikezoe, G. Washino, T. Uemura, S. Kitagawa, H. Matsui, *Nat. Mater.* **2012**, *11*, 1081.
- [10] G. Wang, Z. Xu, Z. Chen, W. Niu, Y. Zhou, J. Guo, L. Tan, *Chem. Comm.* **2013**, *49*, 6641.
- [11] a) U. Mueller, M. Schubert, F. Teich, H. Puetter, K. Schierle-Arndt, J. Pastre, *J. Mater. Chem.* **2006**, *16*, 626; b) A. Kuc, A. Enyashin, G. Seifert, *J. Phys. Chem. B* **2007**, *111*, 8179.
- [12] W. D. Callister, *Materials Science and Engineering: An Introduction*, Wiley, New York **2007**.
- [13] F. Mannone, *Safety in Tritium Handling Technology*, Kluwer Academic Publishers, Luxembourg **1993**.
- [14] A. Carne-Sanchez, I. Imaz, M. Cano-Sarabia, D. Maspoch, *Nat. Chem.* **2013**, *5*, 203.
- [15] B. L. Chen, S. Q. Ma, F. Zapata, F. R. Fronczek, E. B. Lobkovsky, H. C. Zhou, *Inorg. Chem.* **2007**, *46*, 1233.
- [16] O. M. Yaghi, M. O'Keeffe, N. W. Ockwig, H. K. Chae, M. Eddaoudi, J. Kim, *Nature* **2003**, *423*, 705.
- [17] S. Bundschuh, O. Kraft, H. K. Arslan, H. Gliemann, P. G. Weidler, C. Woll, *Appl. Phys. Lett.* **2012**, *101*.
- [18] H. K. Arslan, O. Shekhah, J. Wohlgemuth, M. Franzreb, R. A. Fischer, C. Woll, *Adv. Funct. Mater.* **2011**, *21*, 4228.